

# Altered Corticostriatal Functional Connectivity in Obsessive-compulsive Disorder

Ben J. Harrison, PhD; Carles Soriano-Mas, PhD; Jesus Pujol, MD; Hector Ortiz, MS; Marina López-Solà, BSc; Rosa Hernández-Ribas, MD; Joan Deus, PhD; Pino Alonso, MD; Murat Yücel, PhD; Christos Pantelis, MD; José M. Menchon, MD; Narcís Cardoner, MD

**Context:** Neurobiological models of obsessive-compulsive disorder (OCD) emphasize disturbances in the function and connectivity of brain corticostriatal networks, or “loops.” Although neuroimaging studies of patients have supported this network model of OCD, very few have applied measurements that are sensitive to brain connectivity features.

**Objective:** Using resting-state functional magnetic resonance imaging, we tested the hypothesis that OCD is associated with disturbances in the functional connectivity of primarily ventral corticostriatal regions, measured from coherent spontaneous fluctuations in the blood oxygenation level-dependent (BOLD) signal.

**Design:** Case-control cross-sectional study.

**Setting:** Hospital referral OCD unit and magnetic resonance imaging facility.

**Participants:** A total of 21 patients with OCD (10 men, 11 women) and 21 healthy control subjects matched for age, sex, and estimated intelligence.

**Main Outcome Measures:** Voxelwise statistical parametric maps testing the strength of functional connectivity of 4 striatal seed regions of interest (dorsal caudate

nucleus, ventral caudate/nucleus accumbens, dorsal putamen, and ventral putamen) with remaining brain areas.

**Results:** For both groups, there was a clear distinction in the pattern of cortical connectivity of dorsal and ventral striatal regions, consistent with the notion of segregated motor, associative, and limbic corticostriatal networks. Between groups, patients with OCD had significantly increased functional connectivity along a ventral corticostriatal axis, implicating the orbitofrontal cortex and surrounding areas. The specific strength of connectivity between the ventral caudate/nucleus accumbens and the anterior orbitofrontal cortex predicted patients' overall symptom severity ( $r^2=0.57$ ;  $P<.001$ ). Additionally, patients with OCD showed evidence of reduced functional connectivity of the dorsal striatum and lateral prefrontal cortex, and of the ventral striatum with the region of the midbrain ventral tegmental area.

**Conclusions:** This study directly supports the hypothesis that OCD is associated with functional alterations of brain corticostriatal networks. Specifically, our findings emphasize abnormal and heightened functional connectivity of ventrolimbic corticostriatal regions in patients with OCD.

*Arch Gen Psychiatry.* 2009;66(11):1189-1200

THE BASAL GANGLIA HAVE long been implicated in the pathophysiology of obsessive-compulsive disorder (OCD)<sup>1-3</sup> and remain central to its contemporary neurobiological models.<sup>4</sup> Existing ideas of their dysfunction in OCD have emerged, in particular, through knowledge of basal ganglia-thalamocortical circuits, or “loops,”<sup>5</sup> referring to segregated sensorimotor, associative, and limbic territories of the basal ganglia implicated in motor, cognitive, and emotional aspects of behavior, respectively.<sup>6</sup> In OCD, it has been hypothesized that alterations occurring mostly along a ventral corticostriatal axis may underlie its core symptomatology and even its response to treatments.<sup>7</sup> However, despite the broad appeal of this hypothesis, a de-

finite account of such alterations has not been reached.

A major source of empirical support for neurobiological models of OCD has come from in vivo imaging studies with positron emission tomography (PET) and from structural and functional magnetic resonance imaging (fMRI). Evidence of brain structural alterations implicate the orbitofrontal, anterior cingulate, and temporo- limbic cortices as well as striatal and thalamic subregions, although results have varied across studies.<sup>8</sup> By comparison, heightened activity in the orbitofrontal cortex and caudate nuclei has been well replicated in PET studies of patients at rest<sup>7,9</sup> and, in several instances, predicted symptom severity and normalized following successful treatment.<sup>10-14</sup> A similar pattern has been observed in PET and fMRI studies of

Author Affiliations are listed at the end of this article.

symptom provocation, either in symptomatically mixed groups of patients with OCD<sup>15-20</sup> or among specific subtypes.<sup>21-25</sup> Finally, reduced functional responsiveness of ventral corticostriatal regions, including the orbitofrontal cortex, has been reported in fMRI studies of reversal learning and inhibitory control,<sup>26-29</sup> whereas heightened activation of the dorsal anterior cingulate cortex is evident during response conflict tasks.<sup>30-32</sup>

While existing imaging study has converged in support of a corticostriatal involvement in this disorder, it is important to consider the methodological constraints of such approaches, particularly regarding their spatio-temporal resolution and measurement. In the latter case, this refers to the predominant use of statistical tools to resolve imaging differences (eg, patient vs control) at a voxel-by-voxel or intraregional level, thereby ignoring interrelationships or interactions between brain regions. However, recent advances make it possible to consider the use of alternative mapping techniques<sup>33,34</sup> including those that provide measurements sensitive to brain connectivity features.<sup>35-39</sup> This is relevant both to the study of OCD and to the basal ganglia in general.

Central to this study are recent observations of corticostriatal networks made with resting-state fMRI,<sup>40</sup> a rapidly growing technique that involves the assessment of coherent spontaneous fluctuations of the blood oxygenation level-dependent (BOLD) signal.<sup>41</sup> Compared with conventional task-based studies, resting-state fMRI provides a more sensitive measurement of functional connectivity in large-scale brain networks in humans.<sup>42,43</sup> For instance, as in anatomical models,<sup>5,6</sup> this recent study of the basal ganglia<sup>40</sup> confirmed several predictions about the cortical connectivity of striatal structures including strong evidence of postulated cognitive and affective divisions between areas of the dorsal and ventral striatum. The aim of our study was to add to this work by testing the "corticostriatal loop" hypothesis of OCD.<sup>4,7,44</sup> Based on such theoretical models, in which it is suspected that elevated neuronal excitability may emerge in ventrolimbic corticostriatal networks, we predicted that patients with OCD would show increased functional connectivity between such regions, implicating, in particular, the orbitofrontal cortex. Further, based on early PET studies and other recent fMRI findings,<sup>26</sup> we expected that patients' illness severity would correlate directly with evidence of brain functional alteration.

## METHODS

### PARTICIPANTS

Twenty-four outpatients with OCD were recruited for this study through their ongoing contact with the OCD service at the Department of Psychiatry, University Hospital of Bellvitge, Barcelona, Spain. All patients were required to satisfy *DSM-IV* diagnostic criteria for OCD in the absence of relevant medical, neurological, or other major psychiatric illness.<sup>45</sup> A primary diagnosis of OCD was given if (1) OCD symptoms were the primary reason patients were seeking medical intervention, and (2) OCD symptoms were persistent and constituted the primary cause of distress and interference in the patient's life. No patient met criteria for Tourette's syndrome or had a history of psychoactive drug use and/or abuse. Comorbid anxious and

depressive symptoms were not considered as an exclusion criterion, provided that OCD was the primary clinical diagnosis.

The Yale-Brown Obsessive-Compulsive Scale (YBOCS)<sup>46</sup> and a clinician-rated Yale-Brown Obsessive-Compulsive Scale symptom checklist<sup>46</sup> were used to assess illness severity and to characterize OCD phenomena<sup>47</sup> (**Table 1**). Comorbid symptoms of depression and anxiety were measured by the Hamilton Depression<sup>48</sup> and Anxiety<sup>49</sup> Inventories. All patients were taking stable doses of medication during at least a 3-month period coinciding with the time of the scan, except for 1 patient who was free of medication for at least 1 month (Table 1).

Of the original sample, 3 patients were excluded from the final analysis: 1 male patient owing to an incidental finding on MRI (medial wall hyperintensity) and 2 female patients because of excessive movement during scanning (>2 mm in z-axis translation). The remaining 21 patients were matched for age, sex, handedness, and estimated intelligence quotient to a sample of 21 healthy control subjects (case-matched prior to analyses from a larger cohort identified through an ongoing research program) such that there were no significant group differences on any of these measures (Table 1). General intelligence was estimated using the vocabulary subtest of the Wechsler Adult Intelligence Scale.<sup>50</sup> These sample characteristics were compared between the groups using univariate analyses of variance in Statistical Package for the Social Sciences (SPSS) version 11.0 (SPSS Inc, Cary, North Carolina). Each control subject took the Structured Clinical Interview for *DSM-IV* nonpatient version<sup>51</sup> to exclude any axis I or II psychiatric disorders. No patient in this cohort had a personal history of neurological or psychiatric illness. All participants had normal or corrected-to-normal vision and gave written informed consent to participate following a complete description of the protocol, which was approved by the institutional review board of the University Hospital of Bellvitge, Barcelona.

### IMAGE ACQUISITION AND PREPROCESSING

Images were acquired with a 1.5-T Signa Excite system (General Electric, Milwaukee, Wisconsin) equipped with an 8-channel phased-array head coil and single-shot echoplanar imaging software. Functional sequences consisted of gradient-recalled acquisition in the steady state (time of repetition, 2000 milliseconds; time of echo, 50 milliseconds; pulse angle, 90°) within a field of view of 24 cm, with a 64 × 64 pixel matrix and a slice thickness of 4 mm (interslice gap, 1 mm). Twenty-two interleaved slices parallel to the anterior-posterior commissure line were acquired to cover the whole brain. The first 4 (additional) images were discarded to allow the magnetization to reach equilibrium. For each subject, a single 4-minute continuous functional sequence was acquired, generating 120 whole-brain echoplanar imaging volumes. Subjects were instructed to relax, stay awake, and lie still without moving while keeping their eyes closed throughout. We also acquired a high-resolution T1-weighted anatomical image for each subject using a 3-dimensional fast spoiled gradient inversion-recovery prepared sequence with 130 contiguous slices (time of repetition, 11.8 milliseconds; time of echo, 4.2 milliseconds; flip angle, 15°; field of view, 30 cm; 256 × 256 pixel matrix; slice thickness, 1.2 mm).

Imaging data were transferred and processed on a Microsoft Windows platform running MATLAB version 7 (The MathWorks Inc, Natick, Massachusetts). Image preprocessing was performed in Statistical Parametric Mapping 5 (SPM5) (<http://www.fil.ion.ucl.ac.uk/spm/>). Motion correction was performed by aligning (within subject) each time series to the first image volume using a least-squares minimization and a 6-parameter (rigid body) spatial transformation. These realigned functional sequences were then coregistered to each subject's respective anatomical scan that had been previously coregis-

**Table 1. Sample Characteristics of Healthy Controls and Patients With OCD**

Characteristic	Mean (SD)	Range	
<b>Controls (n=21)</b>			
Age, y	26.2 (3.4)	21-33	
Sex, M:F, No.	10:11		
Handedness, right:left, No.	19:2		
WAIS vocabulary, scaled score	11.71 (1.9)	10-14	
HAM-D	2.8 (3.7)	0-13	
HAM-A	4.8 (5.2)	0-17	
<b>Patients (n=21)<sup>a</sup></b>			
Age, y	28.52 (5.9)	19-39	
Sex, M:F, No.	10:11		
Handedness, right:left, No.	19:2		
WAIS vocabulary, scaled score	12.43 (1.8)	9-16	
Age at onset of OCD, y	20.4 (6.7)	9-34	
Duration of illness, y	8.7 (5.7)	2-28	
Y-BOCS, total	20.7 (6.3)	11-36	
Y-BOCS, obsessions	10.5 (3.2)	5-18	
Y-BOCS, compulsions	10.2 (3.6)	2-18	
HAM-D <sup>b</sup>	7.6 (4.7)	0-19	
HAM-A <sup>b</sup>	11.2 (5.7)	2-21	
<b>No. (%)</b>			
OCD symptom dimensions <sup>c</sup>	<b>0 (Absent)</b>	<b>1 (Mild)</b>	<b>2 (Prominent)</b>
Symmetry, ordering	14 (66.7)	3 (14.3)	4 (19)
Hoarding	15 (71.4)	6 (28.6)	0 (0)
Contamination, cleaning	11 (52.4)	6 (28.6)	4 (19)
Aggressive, checking	5 (23.8)	3 (14.3)	13 (61.9)
Sexual, religious obsessions	16 (76.2)	1 (4.8)	4 (19)
Treatment status			
Never treated with an SSRI		7 (33.3)	
1 Previous SSRI trial		5 (23.8)	
2 Previous SSRI trials		6 (28.6)	
>3 Previous SSRI trials		3 (14.3)	
Previous low-dose antipsychotic use		5 (23.8)	
Cumulative SSRI treatments, mean (SD)		1.33 (1.28)	
Medication at study time			
Medication free (>4 wk)		1 (4.8)	
Fluoxetine		4 (19)	
Fluvoxamine		2 (9.5)	
Citalopram		1 (4.8)	
Clomipramine		2 (9.5)	
Clomipramine with SSRI		11 (52.4)	

Abbreviations: HAM-A, Hamilton Rating Scale for Anxiety; HAM-D, Hamilton Rating Scale for Depression; OCD, obsessive-compulsive disorder; SSRI, selective serotonin reuptake inhibitor; WAIS, Wechsler Adult Intelligence Scale; Y-BOCS, Yale-Brown Obsessive-Compulsive Scale.

<sup>a</sup>The single unmedicated patient with OCD recorded a total Y-BOCS score of 15 and was unremarkable across the other clinical domains.

<sup>b</sup> $P < .001$ . Significant difference between controls and patients.

<sup>c</sup>The Y-BOCS symptom checklist was used to derive scores on 5 previously identified obsessive-compulsive symptom dimensions: symmetry/ordering, hoarding, contamination/cleaning, aggression/checking, and sexual/religious obsessions, classified as absent, present (mild), or prominent.<sup>47</sup>

tered to the SPM-T1 template. Anatomical scans were segmented and normalized to the SPM-T1 template by the unified segmentation approach.<sup>52</sup> Normalization parameters were applied to the coregistered functional images and resliced to 2 mm isotropic resolution. Functional images were smoothed with an 8 mm (full-width, half-maximum) Gaussian filter. With this preprocessing strategy, we ensured that functional scans were in identical stereotaxic (Montreal Neurological Institute) space as the anatomical segments of gray matter, white matter, and cerebrospinal fluid (CSF). All image sequences were routinely inspected for potential normalization artifacts.

### FUNCTIONAL CONNECTIVITY ANALYSES

To assess potential differences in the pattern of cortical and sub-cortical functional connectivity of specific striatal subdivi-

sions of the basal ganglia (caudate nucleus and putamen) between patients with OCD and control subjects, we performed a detailed seed-based cross-correlation analysis of subjects' resting-state imaging sequences. Our approach was based on the method of Di Martino et al<sup>40</sup> and focused on the segregation of functional connectivity maps between the dorsal and ventral striatum. Dorsal and ventral striatal subregions were distinguished using  $z < 7$  mm as a marker for the ventral caudate/nucleus accumbens,  $z > 7$  mm as a marker for dorsal caudate, and  $z = 2$  as the boundary between the dorsal and ventral putamen. These dorsal/ventral borders were initially assigned by Postuma and Dagher<sup>53</sup> from the human stereotaxic atlas of Mai et al<sup>54</sup> and have shown good face validity in human functional connectivity mapping studies.<sup>40,53,55</sup>

Respective seed placements of interest corresponded to the following locations: (1) the dorsal caudate ( $x = \pm 13, y = 15, z = 9$ );

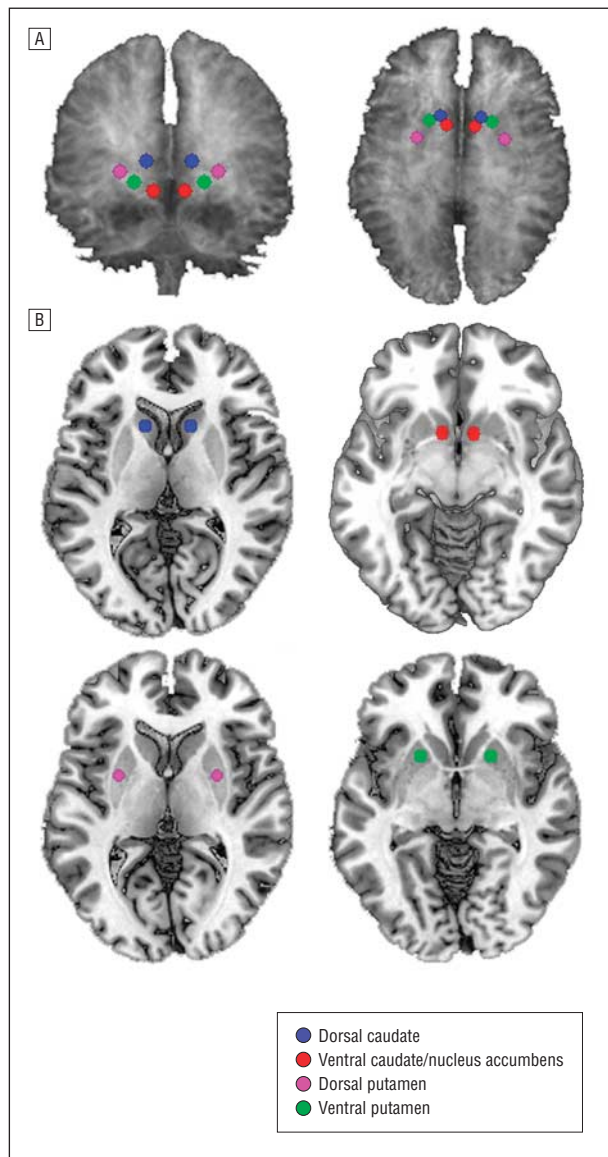


**Figure 1.** Placement of the striatal seed regions of interest on 3-dimensional (A) and 2-dimensional (B) anatomical images. Seeds are presented on a high-resolution single-subject magnetic resonance image in standard neuroanatomical space (Montreal Neurological Institute, Colin-27 template).

(2) the ventral caudate (inferior), corresponding approximately to the nucleus accumbens ( $x = \pm 9, y = 9, z = -8$ ); (3) the dorsal caudal putamen ( $x = \pm 28, y = 1, z = 3$ ); and (4) the ventral rostral putamen ( $x = \pm 20, y = 12, z = -3$ ). To reproduce the finding of segregated dorsal and ventral striatal functional connectivity maps,<sup>40</sup> we included in the model 2 intermediate seeds (of no interest) located in the ventral caudate superior ( $x = \pm 10, y = 15, z = 0$ ) and dorsal rostral putamen ( $x = \pm 25, y = 8, z = 6$ ). This replicated the striatal parcellation method of Di Martino et al<sup>40</sup> and satisfied our aim to contrast the groups as maximally as possible between the dorsal and ventral striatum. Considering the spatial resolution and smoothing of the fMRI data, no seed placements were made in the globus pallidus, substantia nigra, or subthalamic nucleus, as previously discussed.<sup>40</sup> **Figure 1** illustrates the 4 sets of striatal seed regions of interest on 3- and 2-dimensional anatomical images.

For each of the striatal locations, seeds were defined in both hemispheres as 3.5-mm radial spheres (sampling

approximately 25 voxels in 2 mm of isotropic resolution) with a minimum Euclidean distance requirement of 8 mm between any 2 regions.<sup>40</sup> This was performed using MarsBaR region-of-interest toolbox in Montreal Neurological Institute stereotaxic space.<sup>56</sup> Signals were then extracted for each seed (10 in total) by calculating the mean region-of-interest value across the time series. This process was performed for each subject.

In addition to our signals of interest, we derived estimates of white matter, CSF, and global brain signal fluctuations to include in the regression analyses. Subjects' segmented white matter and CSF images were thresholded at 50% tissue probability type and binarized to create nuisance variable masks, together with a binary mask of the global brain volume (summed from the gray matter, white matter, and CSF segments). Nuisance signals were then extracted for each mask by calculating the mean region-of-interest value across the time series. These nuisance signals are typically adjusted for in resting-state functional connectivity studies because they reflect global signal fluctuations of nonneuronal origin (eg, physiological artifacts associated with variables such as cardiac and respiratory cycles, CSF motion, and scanner drift).<sup>41</sup>

## STATISTICAL ANALYSIS

Functional connectivity maps were estimated for each striatal region by including the seed and nuisance signals as predictors of interest or no interest in whole-brain, linear regression analyses in SPM5. These subjectwise (first-level) analyses were carried out separately for each hemisphere. A high-pass filter set at 128 seconds was used to remove low-frequency drifts of less than approximately 0.008 Hz. Prior to model estimation, each of the 3 nuisance covariates were orthogonalized (using an iterative Gram-Schmidt method) and then removed from each seed's time series by linear regression, resulting in a general linear model that comprised the 6 "noise-cleaned" seeds and 3 orthogonal nuisance variables. Contrast images were generated for each subject by estimating the regression coefficient between all brain voxels and each seed's time series, respectively. These images were then included in group (second-level) random-effects analyses, adopting a  $2 \times 2$  mixed design, factorial model (group [control, patient] by hemisphere [right seed, left seed]).

To assess the magnitude and extent of functional connectivity for each striatal seed within groups, resulting z-transformed (Gaussianized) SPMs were thresholded using a false discovery rate correction<sup>57</sup> of  $P_{FDR} < .05$  for the whole-brain volume with a minimum cluster extent of 8 contiguous voxels. Between-group analyses (main effects of group and group  $\times$  hemisphere interactions) were performed by implicitly masking T contrasts (1-tailed) with a global conjunction of these within-group SPMs for both patients and controls. Between-group contrasts were thresholded at  $P < .001$  (uncorrected; minimum cluster extent, 8 contiguous voxels) to more fully characterize the anatomy of functional connectivity differences.

## RESULTS

Overall, both groups exhibited robust and significant patterns of functional connectivity with the 4 striatal seed regions of interest that reproduced the spatial topography of these networks, described by Di Martino and colleagues.<sup>40</sup> This included clear evidence of segregation in the cortical connectivity of the dorsal and ventral cau-

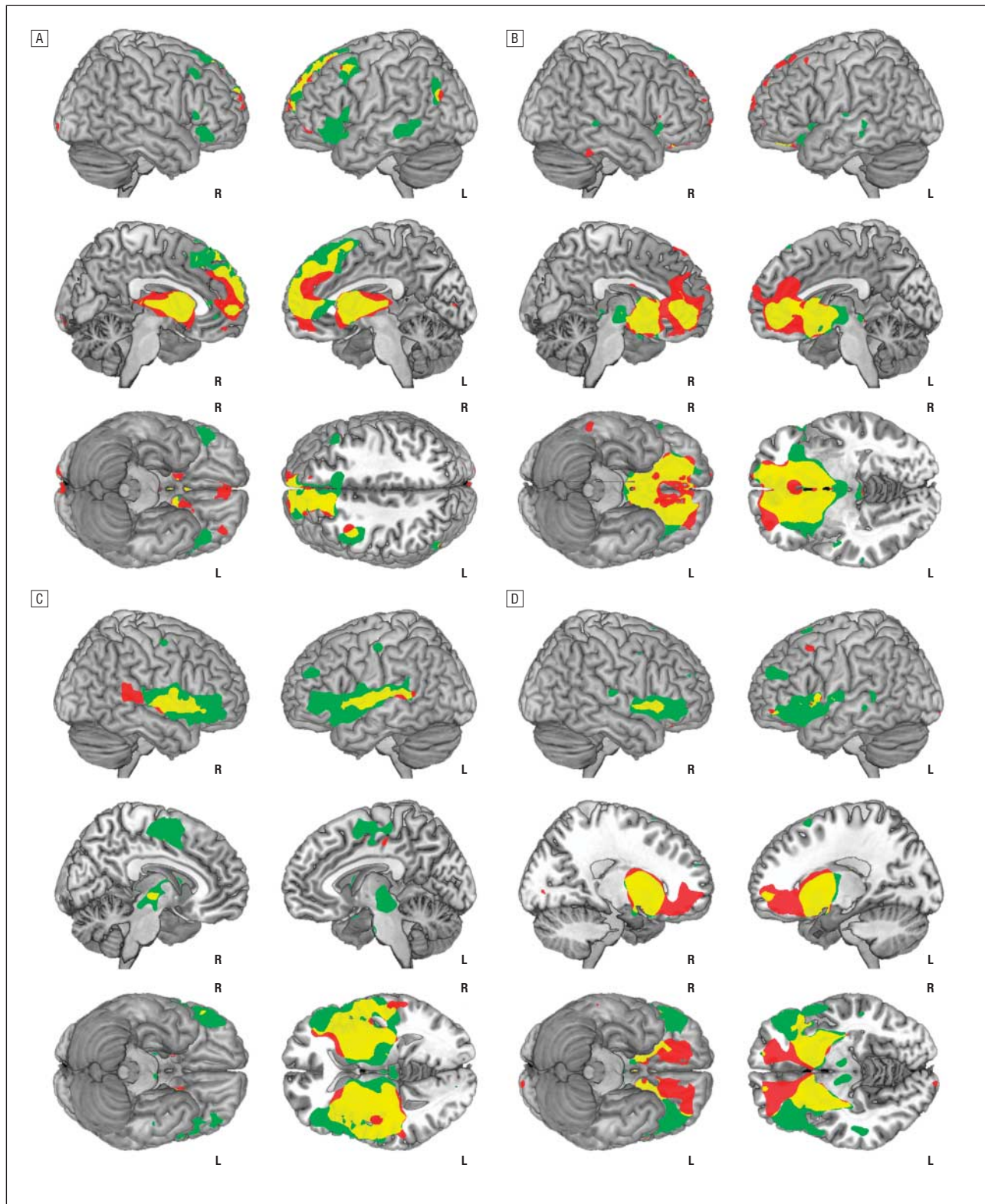


**Figure 2.** Significant within-group (main effect) corticostriatal functional connectivity maps of the dorsal caudate (A), ventral caudate/nucleus accumbens (B), dorsal putamen (C), and ventral putamen (D) seeds. Green indicates control subjects; red, patients with obsessive-compulsive disorder; yellow, the relative spatial overlap of functional connectivity maps between the groups; R, right hemisphere; and L, left hemisphere. Sagittal slices are displayed at  $x = \pm 5$  (A);  $x = \pm 5$  (B);  $x = \pm 7$  (C); and  $x = \pm 18$  (D). Axial slices are displayed at  $z = 45$  (A);  $z = -3$  (B);  $z = 3$  (C); and  $z = -7$  (D). Results are displayed at  $P_{FDR} < .05$ , corrected.

date, and of the dorsal and ventral putamen as quantified in their study (**Figure 2; Table 2**). The specific within- and between-group findings for each of the striatal seed regions are described below.

#### DORSAL CAUDATE REGION

The dorsal caudate seed region in both groups showed significant functional connectivity with the dorsal

**Table 2. Regions Demonstrating Significant Functional Connectivity With the 4 Striatal Seeds of Interest**

Seed	Connected Region <sup>a</sup>	Controls			Patients			Difference <sup>d</sup>							
		Anatomy <sup>b</sup>		Statistic <sup>c</sup>	Anatomy		Statistic	Direction	Anatomy		Statistic				
		x, y, z	z Score	BA	x, y, z	z Score	BA		x, y, z	z Score	BA				
DC	Medial frontal gyrus	0, 65, 19	6.02	10	-8, 62, 3	5.47	10								
		-12, 53, 5	5.60	10											
		-6, 49, 40	5.53	8											
	Superior frontal gyrus	-8, 38, 48	5.51	8									-16, 30, 48	5.15	8
		-8, 32, 57	5.22	6									20, 22, 54	3.04	6
	Pre-SMA	12, 23, 38	4.35	32											
	Inferior frontal gyrus	-30, 21, -3	4.79	47											
	Thalamus (dorsomedial)												-4, -15, 8	5.44	
	Middle frontal gyrus	-40, 14, 51	4.66	6									-36, 50, -7	4.59	10
		46, 27, 41	3.73	8									-40, 14, 44	4.39	6
	Medial temporal gyrus	-58, -30, -3	4.44	21											
	Superior parietal lobe	-51, -64, 38	3.94	39									-48, -67, 27	3.71	39
	Occipital lobe												14, -101, 1	4.06	18
Globus pallidus	-12, 2, 5	7.52		-12, 2, 5	7.37										
	14, 4, 5	6.27		14, 4, 5	7.15										
VC	Orbital frontal gyrus	-16, 48, -10	6.47	10	-18, 40, -7	6.94	10	OCD > HC	-19, 25, -4	3.24	47				
		16, 60, -6	5.42	10	-6, 47, -2	5.32	10	OCD > HC	-10, 60, 24	3.65	10				
		-30, 31, -8	6.29	47	14, 64, -4	4.05	10	OCD > HC	-29, 49, 3	3.45	47				
		20, 34, -10	5.38	47	-10, 67, 10	3.87	10								
					-18, 50, -11	7.03	11								
					-20, 36, -10	6.81	11								
					24, 50, -11	4.95	11								
					18, 58, -4	3.82	11								
	Anterior cingulate gyrus	-8, 33, -1	6.35	24	4, 35, 4	5.44	24	OCD > HC	-7, 27, 34	3.20	32				
		14, 40, -8	6.17	32	8, 46, 27	3.75	32	OCD > HC	-8, 24, -6	3.09	24				
					-8, 42, 16	4.29	32								
	Brainstem (~ VTA)	2, -12, -4	4.92					HC > OCD	-5, -16, -5	3.02					
	Thalamus (pulvinar)	-4, -29, 0	4.29												
Superior temporal gyrus	-49, -11, 4	3.92	22												
Middle temporal gyrus	59, -33, 2	3.88	22				HC > OCD	51, -36, 4	3.47	22					
Globus pallidus	-12, 7, -5	<8		-12, 7, -5	<8										
	12, 7, -5	<8		12, 7, -5	<8										
SN/STN	8, -12, -3	3.71													
	-8, 11, -4	3.37													
DP	Superior frontal gyrus/SMA	4, 5, 51	5.34	6	-10, -3, 48	3.15	6								
		8, 0, 60	5.09		-4, -17, 46	3.47	6								
	Precentral/postcentral gyrus	50, -1, 52	4.69	6	-12, -1, 64	3.19	6								
		-49, -11, 47	3.91	4											
		-23, -30, 59	4.13	3											
Insula cortex	20, -28, 62	3.82	3												
	32, 17, -2	6.72		36, 17, 5	6.38	13									
				-38, 15, 7	6.01	13									
				-49, -4, 7	5.41	6									
				49, 0, 5	5.36	44									
Superior temporal gyrus	53, 8, -4	7.08	22	-51, -25, 8	4.76	41									
	-53, 0, -2	7.00	22	58, -39, 12	4.51	22									
Middle temporal gyrus				-55, -47, 6	3.55	21									
Thalamus (ventrolateral)	-14, -19, 3	7.74		-18, -26, 3	5.32		HC > OCD	-22, -21, 13	3.62						
	14, -15, 3	5.81		8, -13, 1	4.04		HC > OCD	10, -14, 12	3.09						
Brainstem (PAG)	-8, -22, -4	6.85					HC > OCD	-6, -27, -11	4.32						
Inferior frontal gyrus	44, 11, -6	7.42	47	-38, 24, 10	4.12	13	HC > OCD	-43, 32, 7	3.14	46					
	-46, 13, -2	6.27	47	49, 28, 1	3.63	45	HC > OCD	51, 33, 8	3.86	46					
Globus pallidus	24, -6, 2	<8		20, -2, -2	<8										
	-22, -4, 2	<8		-22, -4, -4	<8										
SN/STN	-12, -16, -3	6.03		12, -10, -1	3.99										
	10, -16, -3	5.82		-12, -16, -3	3.05										

(continued)

medial frontal, dorsal premotor (including presupplementary motor and frontal-eye field areas), lateral and inferior frontal cortex, dorsal anterior cingulate, and superior parietal cortices (Figure 2A). No significant differences in the main effect of striatal seed region were seen between control subjects and

patients with OCD for the dorsal caudate seed, although a significant group × hemisphere interaction was observed for the right dorsolateral prefrontal cortex (controls > patients; x, y, z = 36, 41, 35; z score, 3.49; Brodmann area, 9; eFigure 1A; <http://www.archgenpsychiatry.com>).

**Table 2. Regions Demonstrating Significant Functional Connectivity With the 4 Striatal Seeds of Interest (continued)**

Seed	Connected Region <sup>a</sup>	Controls			Patients			Difference <sup>d</sup>				
		Anatomy <sup>b</sup>		Statistic <sup>c</sup>	Anatomy		Statistic	Direction	Anatomy		Statistic	
		x, y, z	z Score		BA	x, y, z			z Score	BA	x, y, z	z Score
VP	Superior frontal gyrus/pre-SMA	0, 5, 53	4.66	6	22, 48, -5	5.38	10					
		22, 53, 18	3.16	10	-4, 15, 56	4.21	6					
	Middle/inferior frontal gyrus	-32, 46, 20	4.43	10	-18, 38, -12	5.80	11	HC > OCD	-34, 27, -1	3.87	47	
		-40, 4, 40	3.44	6	30, 46, 20	3.02	10	HC > OCD	-35, 30, 30	3.53	9	
		51, 20, 41	3.32	8								
		4, -17, 52	3.63	6								
	Inferior frontal gyrus				-16, 34, -12	5.63	47	OCD > HC	-16, 27, -4	3.89	47	
	Precentral gyrus	48, -7, 43	4.66	4	48, -11, 43	3.25	4					
	Medial frontal gyrus				18, 48, -9	5.47	10	OCD > HC	16, 40, -2	3.39	32	
					-20, 50, -7	5.40	10					
	Superior temporal gyrus	-49, -27, 0	4.26	22	-55, 10, 3	3.89	22					
		59, -19, 10	3.55	42								
	Inferior temporal gyrus				59, -32, -22	3.18	20					
	Hippocampus				34, -20, -8	3.42						
	Thalamus (posterior medial)				-16, -21, 1	3.52						
	Brainstem (~ VTA)	4, -14, -14	4.31					HC > OCD	-1, -13, -11	4.20		
	Globus pallidus	-14, 4, 4	<8		-14, 4, 4	<8		HC > OCD	25, -17, 5	3.65		
		12, 4, 1	7.66		12, 4, 1	<8						
	SN/STN	6, -13, 0	4.05		8, -15, -1	3.05						
		-8, -14, -6	4.05									

Abbreviations: BA, Brodmann area; DC, dorsal caudate; DP, dorsal putamen; HC, healthy controls; OCD, obsessive-compulsive disorder; PAG, periaqueductal gray; SMA, supplementary motor area; SN/STN, substantia nigra/subthalamic nucleus; VC, ventral caudate; VP, ventral putamen; ~ VTA, region of the ventral tegmental area.

<sup>a</sup>The strength of effects for the globus pallidus and STN/SN were estimated by performing a small volume search for these structures using masks generated from the Wake Forest University WFU PickAtlas (<http://www.fmri.wfubmc.edu/cms/software/PickAtlas>).

<sup>b</sup>Activity coordinates (x, y, z) are given in Talairach & Tournoux Atlas space. Imaging coordinates were transformed from Statistical Parametric Mapping Montreal Neurological Institute to Talairach space using the Brett transform implemented in GingerALE (<http://www.brainmap.org>). The same conversion applies for all connectivity results reported in text.

<sup>c</sup>Magnitude and extent statistics correspond to a minimum (whole-brain) corrected threshold of  $P_{FDR} < .05$ .

<sup>d</sup>Results correspond to between-group main effect differences thresholded at  $P < .001$ , uncorrected.

### VENTRAL CAUDATE/NUCLEUS ACCUMBENS REGION

The ventral caudate/accumbens seed region in both groups demonstrated significant functional connectivity, primarily with the medial and lateral orbitofrontal cortex and the anterior prefrontal and perigenual (subgenual and rostral) anterior cingulate cortex (Figure 2B). As a main effect of striatal seed region, control subjects demonstrated relatively greater functional connectivity of the ventral caudate/accumbens to the region of the brainstem ventral tegmental area (Figure 3A) and right medial temporal lobe. By comparison, patients demonstrated relatively greater functional connectivity of the ventral caudate/accumbens to the medial orbitofrontal cortex (anterior and posterior clusters) and anterior prefrontal and perigenual (subgenual and dorsal rostral) anterior cingulate cortex. A significant group  $\times$  hemisphere interaction was observed for the left parahippocampal gyrus (patients > controls; x, y, z = -36, -6, -10; z score, 3.91; eFigure 1B).

### DORSAL PUTAMEN REGION

The dorsal putamen seed region in both groups showed significant functional connectivity with the primary and secondary motor areas (supplementary motor cortex), thalamus, anterior insula-operculum, inferior frontal cortex, and superior temporal cortex (Figure 2C). As a main effect of seed region, control subjects demonstrated rela-

tively greater functional connectivity of the dorsal putamen to ventrolateral thalamus and inferior prefrontal cortex (Figure 3B). There was no main effect difference for patients with OCD or any group  $\times$  hemisphere interaction for the dorsal putamen region.

### VENTRAL PUTAMEN REGION

The ventral putamen seed region in both groups showed significant functional connectivity with secondary and cingulate motor areas (presupplementary motor area, dorsal anterior cingulate), dorsal anterior and lateral prefrontal cortex, and lateral and medial orbital frontal cortex (Figure 2D). As a main effect of seed region, control subjects demonstrated relatively greater functional connectivity of the ventral putamen to the frontal operculum/inferior frontal cortex and the region of the brainstem ventral tegmental area. Patients demonstrated relatively greater functional connectivity of the ventral putamen to the subgenual anterior cingulate and posterior medial orbital frontal cortex (Figure 3C). There were no significant group  $\times$  hemisphere interactions for the ventral putamen region.

### COMPARISON BETWEEN STRIATAL REGIONS

We performed a specific assessment of the relative strength of functional connectivity of each striatal seed region with the other approximate seed locations between patients

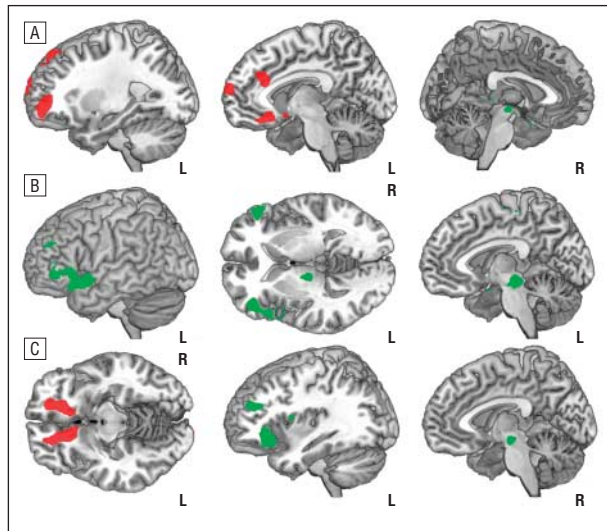


**Figure 3.** Significant between-group (main effect) differences in corticostriatal functional connectivity of the ventral caudate/nucleus accumbens (A), dorsal putamen (B), and ventral putamen (C) seeds. Red overlay corresponds to regions demonstrating greater relative functional connectivity with the respective seed region in patients vs controls; green, regions demonstrating greater relative functional connectivity with the respective seed region in controls vs patients; R, right hemisphere; L, left hemisphere. Slice coordinates are displayed at left  $x = -27$ , center  $x = -8$ , right  $x = 3$  (A); center  $z = 2$ , right  $x = -5$  (B); and left  $z = -10$ ; center  $x = -37$ ,  $x = -5$  (C). Results are displayed at  $P < .001$ , uncorrected.

with OCD and controls. We adopted a more exploratory threshold for this comparison ( $P < .005$ , uncorrected), considering that the spatial extent of correlated regional activities in the proximity of a given functional seed were inevitably highly overlapping between both groups. As a main effect of seed region, patients with OCD demonstrated relatively greater functional connectivity of the dorsal caudate seed with the right ventral caudate/nucleus accumbens ( $x, y, z = 16, 9, -11$ ;  $z$  score, 2.59; eFigure 2A). A group  $\times$  hemisphere interaction was also observed for the left dorsal caudate seed and ventral caudate/nucleus accumbens between patients with OCD and controls (patients  $>$  controls;  $x, y, z = -18, 15, -9$ ;  $z$  score, 2.77; eFigure 2B).

#### BRAIN-BEHAVIORAL ASSOCIATIONS

We performed voxelwise linear regression analyses in SPM5 to test the extent to which patients' overall symptom severity (total YBOCS score) may be related to the strength of functional connectivity among the 4 corticostriatal networks. Only clusters exceeding a threshold of  $P < .001$  (uncorrected) were considered for further post hoc assessment. Across the 4 networks, 1 cluster representing functional connectivity between the ventral striatum to anterior orbital frontal cortex ( $x, y, z = 24, 58, -1$ ) predicted patients' overall symptom severity ( $z$  score, 3.91). Using the volume-of-interest function in SPM5, we extracted the first eigenvariate of all voxel values (contrast  $\beta$  weights) from a 3.5-mm sphere centered on this cluster for each subject. As shown in **Figure 4**, the relative strength of functional connectivity between the ventral striatum and anterior orbital frontal cortex accounted for approximately half of the variance of patients' total YBOCS scores (2-tailed Pearson  $r = 0.76$ ;  $r^2 = 0.57$ ;  $P < .001$ ). This

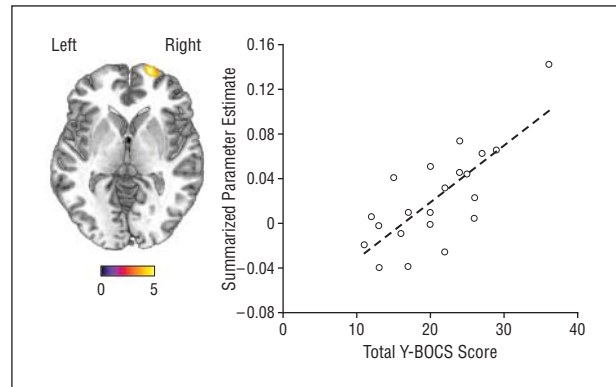


**Figure 4.** Strength of functional connectivity between the ventral striatum and anterior orbital frontal cortex predicted the total Yale-Brown Obsessive-Compulsive Scale (Y-BOCS) scores of patients with obsessive-compulsive disorder ( $P < .001$ ). Axial slice displayed at  $z = 1$ .

relationship remained significant in a partial correlation analysis (2-tailed in SPSS) that controlled for patients' comorbid depression and anxiety ratings on the Hamilton Depression Inventory and Hamilton Anxiety Inventory scales (Pearson  $r = 0.56$ ;  $P < .01$ ).

#### COMMENT

The results of our study provide direct support for the hypothesis that OCD is associated with functional network alterations of the basal ganglia and frontal cortex.<sup>4,7,58,59</sup> More specifically, our study adds to prior imaging findings by showing that such alterations exist as disturbed interrelationships between brain regions, a basic prediction of neurobiological models of OCD.

The topography, or spatial organization, of the 4 functional networks described in our study is in strong agreement with recent MRI studies of human subjects<sup>40,60</sup> and existing neurocircuitry (loop) models of the connective anatomy of the basal ganglia regions.<sup>5,6,61</sup> These results can be considered with the emerging view that spontaneous BOLD signal correlations between distributed brain areas closely parallel, and may be synchronized by, underlying axonal connections.<sup>62,63</sup>

A major difference between patients with OCD and control subjects was observed in the strength of functional connectivity between ventral corticostriatal regions. Specifically, patients had increased functional connectivity between the 2 ventral striatal regions and the medial orbital frontal, anterior frontal, rostral anterior cingulate, and parahippocampal regions. With the exception of parahippocampal cortex, which has shown functional alterations in task-related studies of OCD,<sup>64,65</sup> increased metabolic activity of these regions has been described in studies of patients at rest using PET. However, distinct from such previous work, our findings refer to specific increases in their strength of temporally correlated activity in patients with OCD, which do not necessarily reflect absolute differences in underlying neuronal activity levels.<sup>66</sup>

After controlling for comorbid symptoms, the strength of functional connectivity between the ventral caudate/

nucleus accumbens region and medial orbitofrontal cortex predicted patients' total YBOCS scores, indicating a direct relationship to global illness severity. This result corresponds well with previous PET studies of patients at rest in which orbitofrontal hypermetabolism was identified as a potential biomarker of OCD severity, based on similar linear correlations with clinical measures and its normalization of activity posttreatment.<sup>12-14,67-69</sup> Correlations of this kind have also been reported in symptom provocation studies, in this case related to orbitofrontal hyperactivation above baselines states.<sup>17,20,25</sup> Most recently, orbitofrontal dysfunction was identified in first-degree relatives of patients with OCD, providing strong evidence that it may be a specific vulnerability marker (endophenotype) of illness.<sup>26</sup> Thus, despite the wide variety of methods used, functional imaging studies continue to converge on the role of the orbitofrontal cortex and surrounding areas in OCD.

Neurosurgical procedures for treatment-refractory OCD, in particular with chronic deep-brain stimulation, have shown recent efficacy in targeting the ventral striatum/nucleus accumbens region<sup>70</sup> as well as other sites.<sup>71</sup> Research in animals suggests that the therapeutic mode of action of accumbens deep-brain stimulation may occur via recurrent inhibition of orbitofrontal neurons<sup>72</sup>; however, the role of preexisting striatal dysfunction is presently unknown. We found greater functional connectivity of the dorsal caudate and ventral caudate/accumbens in patients with OCD, which suggests excessive activity coupling between these dorsal and ventral striatal regions—a mechanism that has been linked to other compulsive behaviors.<sup>73</sup> This effect was most prominent in the left hemisphere, which has been noted in some,<sup>74,75</sup> but not other, functional imaging findings in OCD.<sup>10,76</sup> Nonetheless, our observation supports recent findings,<sup>37,74</sup> including a study of elevated and irregular spiking activity of ventral caudate/accumbens neurons in patients with OCD,<sup>75</sup> suggesting that alterations are evident both at the level of the cortex and of the ventral striatum in this disorder.

Patients with OCD had an apparent loss of functional connectivity of the ventral striatal regions and the region of the midbrain ventral tegmental area, an unanticipated finding. Under normal conditions, the latter area provides the former with dense dopaminergic innervation that are presumed to be critical for cortically driven action selection and long-term plasticity of corticostriatal loops.<sup>5,77</sup> While current evidence from *in vivo* studies suggests that striatal dopamine activity may be elevated in patients with OCD, findings have been mixed.<sup>78</sup> Nevertheless, what may be most the relevant aspect of our results is the seemingly homologous nature of the ventral caudate/accumbens network and recent functional connectivity mapping studies of the ascending dopamine system in animals with pharmacological fMRI.<sup>79</sup> Given that empirical interests in the role of dopamine are growing in OCD, translational studies with fMRI are a promising avenue for future work.

While alterations of ventral corticostriatal regions may ultimately express the core pathophysiology of OCD, broader alterations are also frequently identified in patients with OCD, as addressed in a recent comprehensive survey of the imaging literature.<sup>33</sup> As secondary findings, we observed patterns of reduced functional

connectivity of both putamen regions with the frontal operculum/inferior frontal cortex, and the right dorsal caudate nucleus with the right dorsolateral prefrontal cortex in patients with OCD. Taken with the aforementioned results, it is interesting to consider such patterns with the idea of imbalance in corticostriatal loop models of OCD,<sup>7</sup> drawn here as a comparison between the strength of functional connectivity differences in ventral (affective) and dorsal (cognitive) corticostriatal networks in patients with OCD.

Evidence of resting alterations in dorsal and lateral prefrontal regions in OCD has been limited, and existing studies are mostly contradictory.<sup>33</sup> Task-oriented fMRI has had more success in probing higher cortical disturbances in patients with OCD, particularly across domains of executive function,<sup>28,29,31,32,80</sup> consistent with other behavioral findings.<sup>81</sup> However, the results of these imaging studies also vary substantially in terms of the nature of the functional impairments characterized. That is, whereas findings of hyperactivation are often thought to compensate for an underlying neuronal deficit, hypoactivation is typically argued to be direct evidence of such deficits. Both interpretations may, in fact, be misleading if a region or network's ongoing activity fluctuations are disturbed in a patient group. Our findings of cortical resting-state alterations in patients with OCD may, therefore, have implications for future task-related fMRI studies.

Nonneuronal factors contribute to the variance of spontaneous BOLD signal fluctuations. However, mounting evidence suggests that current analysis techniques are able to mitigate their influence.<sup>41,82,83</sup> Indeed, general appreciation of the reliability of resting-state functional connectivity has grown over the past few years, together with insight into the neural basis of this measurement.<sup>41</sup> Recently, evidence was put forward to show that spontaneous BOLD signal correlations between different regions resemble those of spontaneous slow cortical potentials recorded from the electrocorticogram and across distinct arousal states.<sup>84</sup> The overarching inference here is that both signals represent endogenous fluctuations of neuronal excitability within functional brain systems.

Because spontaneous BOLD signal correlations remain evident in reduced states of consciousness, they are suspected to index a fundamental, or intrinsic, traitlike property of the functional organization of the brain.<sup>41</sup> However, these resting-state functional connectivity measurements are also dynamic and can be modulated by moment-to-moment or gradual shifts in arousal and by cognitive or emotional states.<sup>83,85</sup> This raises the question, do the findings of this study reflect a cause or a correlate of patients' symptomatic states? The significant correlation between our connectivity measure and patients' YBOCS scores seems to argue the latter. However, the correspondence of these functional networks to known anatomical connectivities and the fact that such connectivities develop according to distinct maturation rates that may be compromised in OCD<sup>86</sup> suggest that both possibilities may be valid, or at least that this question remains open.

We consider this study a useful starting point for future investigations of resting-state functional connectivity in OCD, in relation to both corticostriatal networks and other large-scale brain systems. In both cases, it will be impor-

tant for such studies to address the multisymptomatic nature of OCD populations in specific detail, as performed in other larger-scale MRI studies.<sup>37,87</sup> While our patients were characterized by more prominent aggressive/checking symptoms, consistent with prior studies,<sup>34</sup> we were unable to perform the appropriate statistical tests (ie, because of sample size) to determine whether our results can be related preferentially to one or another major symptom dimension or generalized to all patients with this disorder. This is a caveat that should be addressed in future work. Additionally, the assessment of patients both taking and not taking medication will also be relevant in further studies of corticostriatal functional networks in OCD. Most patients in our study had completed 1 or more trials of selective serotonin reuptake inhibitor antidepressant treatment. Although based on previous work, chronic selective serotonin reuptake inhibitor treatment in OCD may be expected to normalize heightened resting-state activity in ventral corticostriatal regions<sup>12</sup>; its influence on specific functional connectivity measurements requires investigation.

Resting-state fMRI has obvious practical benefits when studying psychiatric populations,<sup>82</sup> including its ease of use and the fact that reliable brain mapping results can be obtained from relatively brief scanning sessions (<10 minutes).<sup>88</sup> However, despite such benefits, resting-state fMRI should be seen as complementary to task-based imaging studies, as both are likely to be mutually informative. For example, the integration of both approaches may be useful in reconciling the apparently divergent findings of reduced task-related activation<sup>26-29</sup> and heightened resting-state activity and striatal functional connectivity of the orbitofrontal cortex in patients with OCD. Lastly, although we were able to perform whole-brain echoplanar imaging by scanning at 1.5 T, higher-field fMRI with increased sensitivity is likely to improve the level of anatomical description achieved in this study.

While our findings support the prevailing hypothesis that corticostriatal networks are dysfunctional in OCD, the specific neural mechanisms and vulnerability factors that give rise to this impairment remain to be understood. There is strong potential for neuroimaging to generate further insight to this end, especially if combined with current advances in clinical, developmental, and molecular neuroscience studies of OCD.

**Submitted for Publication:** November 12, 2008; final revision received January 26, 2009; accepted March 16, 2009.

**Author Affiliations:** Institut d'Alta Tecnologia-Parc de Recerca Biomèdica de Barcelona, Centro Radiològic Computerizado Corporació Sanitària, Barcelona, Spain (Drs Harrison, Soriano-Mas, Pujol, Hernández-Ribas, Deus, and Cardoner, Ms López-Solà, and Mr Ortiz); Melbourne Neuropsychiatry Centre, Department of Psychiatry, The University of Melbourne & Melbourne Health, Australia (Drs Harrison, Yücel, and Pantelis); Department of Electronic Engineering, Technical University of Catalonia, Barcelona, Spain (Mr Ortiz); Department of Clinical Sciences, Faculty of Medicine, University of Barcelona, Spain (Ms López-Solà); Department of Psychiatry, Bellvitge University Hospital, Centro de Investigación Biomédica en Red de Salud Mental, Barcelona, Spain

(Drs Hernández-Ribas, Alonso, Menchon, and Cardoner); Department of Clinical and Health Psychology, Autonomous University of Barcelona, Barcelona, Spain (Dr Deus); Orygen Research Centre, Melbourne, Australia (Dr Yücel); Networking Research Center on Bioengineering, Biomaterials and Nanomedicine, Centro de Investigación Biomédica en Red en Bioingeniería, Biomaterials y Nanomedicina, Barcelona, Spain (Dr Pujol). **Correspondence:** Ben J. Harrison, PhD, Melbourne Neuropsychiatry Centre, National Neuroscience Facility, 161 Barry St, Carlton, Melbourne, Australia 3053 (habj@unimelb.edu.au).

**Author Contributions:** Dr Harrison had full access to all of the data in the study and takes responsibility for the integrity of the data and the accuracy of the data analysis. **Financial Disclosure:** None reported.

**Funding/Support:** This study was supported in part by the Instituto de Salud Carlos III, Centro de Investigación en Red de Salud Mental, Fondo de Investigación Sanitaria grants PI050884 and PI071029; National Health and Medical Research Council of Australia (NHMRC) Training Award 400420 (Dr Harrison); NHMRC Clinical Career Development Award 509345 (Dr Yücel); the Networking Research Center on Bioengineering, Biomaterials and Nanomedicine, Barcelona, Spain (Dr Pujol); and Formación de Personal Universitario scholarships AP2005-0408 and AP2006-02869 from the Spanish Ministry of Education (Ms López-Solà and Mr Ortiz).

**Additional Information:** The eFigures are available at <http://www.archgenpsychiatry.com>.

## REFERENCES

- Laplane D, Levasseur M, Pillon B, Dubois B, Baulac M, Mazoyer B, Tran Dinh S, Sette G, Danze F, Baron JC. Obsessive-compulsive and other behavioural changes with bilateral basal ganglia lesions: a neuropsychological, magnetic resonance imaging and positron tomography study. *Brain*. 1989;112(pt 3):699-725.
- Modell JG, Mountz JM, Curtis GC, Greden JF. Neurophysiologic dysfunction in basal ganglia/limbic striatal and thalamocortical circuits as a pathogenetic mechanism of obsessive-compulsive disorder. *J Neuropsychiatry Clin Neurosci*. 1989; 1(1):27-36.
- Rapoport JL, Wise SP. Obsessive-compulsive disorder: evidence for basal ganglia dysfunction. *Psychopharmacol Bull*. 1988;24(3):380-384.
- Graybiel AM, Rauch SL. Toward a neurobiology of obsessive-compulsive disorder. *Neuron*. 2000;28(2):343-347.
- Alexander GE, DeLong MR, Strick PL. Parallel organization of functionally segregated circuits linking basal ganglia and cortex. *Annu Rev Neurosci*. 1986; 9:357-381.
- Haber SN. The primate basal ganglia: parallel and integrative networks. *J Chem Neuroanat*. 2003;26(4):317-330.
- Saxena S. Neuroimaging and the pathophysiology of obsessive compulsive disorder. In: Fu C, Senior C, Russell TA, Weinberger DR, Murray R, eds. *Neuroimaging in Psychiatry*. London, England: Martin Dunitz; 2003:191-224.
- Menzies L, Chamberlain SR, Laird AR, Thelen SM, Sahakian BJ, Bullmore ET. Integrating evidence from neuroimaging and neuropsychological studies of obsessive-compulsive disorder: the orbitofronto-striatal model revisited. *Neurosci Biobehav Rev*. 2008;32(3):525-549.
- Whiteside SP, Port JD, Abramowitz JS. A meta-analysis of functional neuroimaging in obsessive-compulsive disorder. *Psychiatry Res*. 2004;132(1):69-79.
- Baxter LR Jr, Schwartz JM, Bergman KS, Szuba MP, Guze BH, Mazziotta JC, Alazraki A, Selin CE, Ferng HK, Munford P, Phelps ME. Caudate glucose metabolic rate changes with both drug and behavior therapy for obsessive-compulsive disorder. *Arch Gen Psychiatry*. 1992;49(9):681-689.
- Baxter LR Jr, Schwartz JM, Mazziotta JC, Phelps ME, Pahl JJ, Guze BH, Fairbanks L. Cerebral glucose metabolic rates in nondepressed patients with obsessive-compulsive disorder. *Am J Psychiatry*. 1988;145(12):1560-1563.
- Saxena S, Brody AL, Maidment KM, Dunkin JJ, Colgan M, Alborzian S, Phelps ME, Baxter LR Jr. Localized orbitofrontal and subcortical metabolic changes and pre-

- dictors of response to paroxetine treatment in obsessive-compulsive disorder. *Neuropsychopharmacology*. 1999;21(6):683-693.
13. Schwartz JM, Stoessel PW, Baxter LR Jr, Martin KM, Phelps ME. Systematic changes in cerebral glucose metabolic rate after successful behavior modification treatment of obsessive-compulsive disorder. *Arch Gen Psychiatry*. 1996;53(2):109-113.
  14. Swedo SE, Pietrini P, Leonard HL, Schapiro MB, Rettew DC, Goldberger EL, Rapoport SI, Rapoport JL, Grady CL. Cerebral glucose metabolism in childhood-onset obsessive-compulsive disorder: reevaluation during pharmacotherapy. *Arch Gen Psychiatry*. 1992;49(9):690-694.
  15. Adler CM, McDonough-Ryan P, Sax KW, Holland SK, Arndt S, Strakowski SM. fMRI of neuronal activation with symptom provocation in unmedicated patients with obsessive compulsive disorder. *J Psychiatr Res*. 2000;34(4-5):317-324.
  16. Breiter HC, Rauch SL, Kwong KK, Baker JR, Weisskoff RM, Kennedy DN, Kendrick AD, Davis TL, Jiang A, Cohen MS, Stern CE, Belliveau JW, Baer L, O'Sullivan RL, Savage CR, Jenike MA, Rosen BR. Functional magnetic resonance imaging of symptom provocation in obsessive-compulsive disorder. *Arch Gen Psychiatry*. 1996;53(7):595-606.
  17. Mataix-Cols D, Wooderson S, Lawrence N, Brammer MJ, Speckens A, Phillips ML. Distinct neural correlates of washing, checking, and hoarding symptom dimensions in obsessive-compulsive disorder. *Arch Gen Psychiatry*. 2004;61(6):564-576.
  18. Schienle A, Schafer A, Stark R, Walter B, Vaitl D. Neural responses of OCD patients towards disorder-relevant, generally disgust-inducing and fear-inducing pictures. *Int J Psychophysiol*. 2005;57(1):69-77.
  19. McGuire PK, Bench CJ, Frith CD, Marks IM, Frackowiak RS, Dolan RJ. Functional anatomy of obsessive-compulsive phenomena. *Br J Psychiatry*. 1994;164(4):459-468.
  20. Rauch SL, Jenike MA, Alpert NM, Baer L, Breiter HC, Savage CR, Fischman AJ. Regional cerebral blood flow measured during symptom provocation in obsessive-compulsive disorder using oxygen 15-labeled carbon dioxide and positron emission tomography. *Arch Gen Psychiatry*. 1994;51(1):62-70.
  21. Phillips ML, Marks IM, Senior C, Lythgoe D, O'Dwyer AM, Meehan O, Williams SC, Brammer MJ, Bullmore ET, McGuire PK. A differential neural response in obsessive-compulsive disorder patients with washing compared with checking symptoms to disgust. *Psychol Med*. 2000;30(5):1037-1050.
  22. Shapira NA, Liu Y, He AG, Bradley MM, Lessig MC, James GA, Stein DJ, Lang PJ, Goodman WK. Brain activation by disgust-inducing pictures in obsessive-compulsive disorder. *Biol Psychiatry*. 2003;54(7):751-756.
  23. Lawrence NS, An SK, Mataix-Cols D, Ruths F, Speckens A, Phillips ML. Neural responses to facial expressions of disgust but not fear are modulated by washing symptoms in OCD. *Biol Psychiatry*. 2007;61(9):1072-1080.
  24. van den Heuvel OA, Veltman DJ, Groenewegen HJ, Dolan RJ, Cath DC, Boellaard R, Mesina CT, van Balkom AJ, van Oppen P, Witter MP, Lammertsma AA, van Dyck R. Amygdala activity in obsessive-compulsive disorder with contamination fear: a study with oxygen-15 water positron emission tomography. *Psychiatry Res*. 2004;132(3):225-237.
  25. Rauch SL, Shin LM, Dougherty DD, Alpert NM, Fischman AJ, Jenike MA. Predictors of fluvoxamine response in contamination-related obsessive compulsive disorder: a PET symptom provocation study. *Neuropsychopharmacology*. 2002;27(5):782-791.
  26. Chamberlain SR, Menzies L, Hampshire A, Suckling J, Fineberg NA, del Campo N, Aitken M, Craig K, Owen AM, Bullmore ET, Robbins TW, Sahakian BJ. Orbitofrontal dysfunction in patients with obsessive-compulsive disorder and their unaffected relatives. *Science*. 2008;321(5887):421-422.
  27. Remijne PL, Nielen MM, van Balkom AJ, Cath DC, van Oppen P, Uylings HB, Veltman DJ. Reduced orbitofrontal-striatal activity on a reversal learning task in obsessive-compulsive disorder. *Arch Gen Psychiatry*. 2006;63(11):1225-1236.
  28. Roth RM, Saykin AJ, Flashman LA, Pixley HS, West JD, Mamourian AC. Event-related functional magnetic resonance imaging of response inhibition in obsessive-compulsive disorder. *Biol Psychiatry*. 2007;62(8):901-909.
  29. van den Heuvel OA, Veltman DJ, Groenewegen HJ, Cath DC, van Balkom AJ, van Hartskamp J, Barkhof F, van Dyck R. Frontal-striatal dysfunction during planning in obsessive-compulsive disorder. *Arch Gen Psychiatry*. 2005;62(3):301-309.
  30. Maltby N, Tolin DF, Worhunsky P, O'Keefe TM, Kiehl KA. Dysfunctional action monitoring hyperactivates frontal-striatal circuits in obsessive-compulsive disorder: an event-related fMRI study. *Neuroimage*. 2005;24(2):495-503.
  31. van der Wee NJ, Ramsey NF, Jansma JM, Denys DA, van Megren HJ, Westenberg HM, Kahn RS. Spatial working memory deficits in obsessive compulsive disorder are associated with excessive engagement of the medial frontal cortex. *Neuroimage*. 2003;20(4):2271-2280.
  32. Yücel M, Harrison BJ, Wood SJ, Fornito A, Wellard RM, Pujol J, Clarke K, Phillips ML, Kyrios M, Velakoulis D, Pantelis C. Functional and biochemical alterations of the medial frontal cortex in obsessive-compulsive disorder. *Arch Gen Psychiatry*. 2007;64(8):946-955.
  33. Menzies L, Achard S, Chamberlain SR, Fineberg N, Chen CH, del Campo N, Sahakian BJ, Robbins TW, Bullmore E. Neurocognitive endophenotypes of obsessive-compulsive disorder. *Brain*. 2007;130(pt 12):3223-3236.
  34. Soriano-Mas C, Pujol J, Alonso P, Cardoner N, Menchon JM, Harrison BJ, Deus J, Vallejo J, Gaser C. Identifying patients with obsessive-compulsive disorder using whole-brain anatomy. *Neuroimage*. 2007;35(3):1028-1037.
  35. Cardoner N, Soriano-Mas C, Pujol J, Alonso P, Harrison BJ, Deus J, Hernandez-Ribas R, Menchon JM, Vallejo J. Brain structural correlates of depressive comorbidity in obsessive-compulsive disorder. *Neuroimage*. 2007;38(3):413-421.
  36. Harrison BJ, Yücel M, Shaw M, Kyrios M, Maruff P, Brewer WJ, Purcell R, Velakoulis D, Strother SC, Scott AM, Nathan PJ, Pantelis C. Evaluating brain activity in obsessive-compulsive disorder: preliminary insights from a multivariate analysis. *Psychiatry Res*. 2006;147(2-3):227-231.
  37. Pujol J, Soriano-Mas C, Alonso P, Cardoner N, Menchon JM, Deus J, Vallejo J. Mapping structural brain alterations in obsessive-compulsive disorder. *Arch Gen Psychiatry*. 2004;61(7):720-730.
  38. Menzies L, Williams GB, Chamberlain SR, Ooi C, Fineberg N, Suckling J, Sahakian BJ, Robbins TW, Bullmore ET. White matter abnormalities in patients with obsessive-compulsive disorder and their first-degree relatives [published online ahead of print June 2, 2008]. *Am J Psychiatry*. 2008;165(10):1308-1315.
  39. Szeszko PR, Ardekani BA, Ashtari M, Malhotra AK, Robinson DG, Bilder RM, Lim KO. White matter abnormalities in obsessive-compulsive disorder: a diffusion tensor imaging study. *Arch Gen Psychiatry*. 2005;62(7):782-790.
  40. Di Martino A, Scheres A, Margulies DS, Kelly AM, Uddin LQ, Shehzad Z, Biswal B, Walters JR, Castellanos FX, Milham MP. Functional connectivity of human striatum: a resting state fMRI study [published online ahead of print April 9, 2008]. *Cereb Cortex*. 2008;18(12):2735-2747.
  41. Fox MD, Raichle ME. Spontaneous fluctuations in brain activity observed with functional magnetic resonance imaging. *Nat Rev Neurosci*. 2007;8(9):700-711.
  42. Damoiseaux JS, Rombouts SA, Barkhof F, Scheltens P, Stam CJ, Smith SM, Beckmann CF. Consistent resting-state networks across healthy subjects. *Proc Natl Acad Sci U S A*. 2006;103(37):13848-13853.
  43. Hampson M, Peterson BS, Skudlarski P, Gatenby JC, Gore JC. Detection of functional connectivity using temporal correlations in MR images. *Hum Brain Mapp*. 2002;15(4):247-262.
  44. Aouizerate B, Guehl D, Cuny E, Rougier A, Bioulac B, Tignol J, Burbaud P. Pathophysiology of obsessive-compulsive disorder: a necessary link between phenomenology, neuropsychology, imagery and physiology. *Prog Neurobiol*. 2004;72(3):195-221.
  45. First MB, Spitzer RL, Gibbon M, Williams JB. *Structured Clinical Interview for DSM-IV Axis 1 Disorders*. Washington, DC: American Psychiatric Press; 1998.
  46. Goodman WK, Price LH, Rasmussen SA, Mazure C, Fleischmann RL, Hill CL, Heninger GR, Charney DS. The Yale-Brown Obsessive Compulsive Scale I: development, use, and reliability. *Arch Gen Psychiatry*. 1989;46(11):1006-1011.
  47. Mataix-Cols D, Rauch SL, Manzo PA, Jenike MA, Baer L. Use of factor-analyzed symptom dimensions to predict outcome with serotonin reuptake inhibitors and placebo in the treatment of obsessive-compulsive disorder. *Am J Psychiatry*. 1999;156(9):1409-1416.
  48. Hamilton M. A rating scale for depression. *J Neurol Neurosurg Psychiatry*. 1960;23:56-62.
  49. Hamilton M. The assessment of anxiety states by rating. *Br J Med Psychol*. 1959;32(1):50-55.
  50. Wechsler D. *Wechsler Abbreviated Scale of Intelligence Manual*. San Antonio, TX: The Psychological Corporation; 1999.
  51. First MB, Spitzer RL, Gibbon M, Williams JB. *Structured Clinical Interview for DSM-IV-RS Axis 1 Disorders: Non-Patient Edition (SCID-I/NP)*. New York, NY: Biometrics Research, New York State Psychiatric Institute; 2007.
  52. Ashburner J, Friston KJ. Unified segmentation. *Neuroimage*. 2005;26(3):839-851.
  53. Postuma RB, Dagher A. Basal ganglia functional connectivity based on a meta-analysis of 126 positron emission tomography and functional magnetic resonance imaging publications. *Cereb Cortex*. 2006;16(10):1508-1521.
  54. Mai J, Assheuer J, Paxinos G. *Atlas of the Human Brain*. San Diego, CA: Academic Press; 1997.
  55. Toro R, Fox PT, Paus T. Functional coactivation map of the human brain. *Cereb Cortex*. 2008;18(11):2553-2559.
  56. Region of interest analysis using an SPM toolbox [abstract]. Brett M, Anton JL, Valabregue R, Poline JB. Presented at: The 8th International conference on Functional Mapping of the Human Brain; June 2-6, 2002; Sendai, Japan. Available on CD-ROM in *Neuroimage* 16(2).
  57. Genovese CR, Lazar NA, Nichols T. Thresholding of statistical maps in functional neuroimaging using the false discovery rate. *Neuroimage*. 2002;15(4):870-878.
  58. Baxter LR Jr. Basal ganglia systems in ritualistic social displays: reptiles and humans; function and illness. *Physiol Behav*. 2003;79(3):451-460.
  59. Schwartz JM. Neuroanatomical aspects of cognitive-behavioural therapy response in obsessive-compulsive disorder: an evolving perspective on brain and behaviour. *Br J Psychiatry Suppl*. 1998;(35):38-44.

60. Draganski B, Kherif F, Klöppel S, Cook PA, Alexander DC, Parker GJ, Deichmann R, Ashburner J, Frackowiak RS. Evidence for segregated and integrative connectivity patterns in the human basal ganglia. *J Neurosci*. 2008;28(28):7143-7152.
61. Groenewegen HJ, Trimble M. The ventral striatum as an interface between the limbic and motor systems. *CNS Spectr*. 2007;12(12):887-892.
62. Greicius MD, Supekar K, Menon V, Dougherty RF. Resting-state functional connectivity reflects structural connectivity in the default mode network [published online ahead of print April 9, 2008]. *Cereb Cortex*. 2009;19(1):72-78.
63. Vincent JL, Patel GH, Fox MD, Snyder AZ, Baker JT, Van Essen DC, Zempel JM, Snyder LH, Corbetta M, Raichle ME. Intrinsic functional architecture in the anesthetized monkey brain. *Nature*. 2007;447(7140):83-86.
64. Rauch SL, Savage CR, Alpert NM, Dougherty D, Kendrick A, Curran T, Brown HD, Manzo P, Fischman AJ, Jenike MA. Probing striatal function in obsessive-compulsive disorder: a PET study of implicit sequence learning. *J Neuropsychiatry Clin Neurosci*. 1997;9(4):568-573.
65. Rauch SL, Wedig MM, Wright CI, Martis B, McMullin KG, Shin LM, Cannistraro PA, Wilhelm S. Functional magnetic resonance imaging study of regional brain activation during implicit sequence learning in obsessive-compulsive disorder. *Biol Psychiatry*. 2007;61(3):330-336.
66. Raichle ME, Mintun MA. Brain work and brain imaging. *Annu Rev Neurosci*. 2006;29:449-476.
67. Benkeffat C, Nordahl TE, Semple WE, King AC, Murphy DL, Cohen RM. Local cerebral glucose metabolic rates in obsessive-compulsive disorder: patients treated with clomipramine. *Arch Gen Psychiatry*. 1990;47(9):840-848.
68. Biver F, Goldman S, Francois A, De La Porte C, Luxen A, Gribomont B, Lotstra F. Changes in metabolism of cerebral glucose after stereotactic leukotomy for refractory obsessive-compulsive disorder: a case report. *J Neurol Neurosurg Psychiatry*. 1995;58(4):502-505.
69. Matsumoto R, Nakamae T, Yoshida T, Kitabayashi Y, Ushijima Y, Narumoto J, Ito H, Suhara T, Fukui K. Recurrent hyperperfusion in the right orbitofrontal cortex in obsessive-compulsive disorder. *Prog Neuropsychopharmacol Biol Psychiatry*. 2008;32(4):1082-1084.
70. Greenberg BD, Gabriels LA, Malone DA Jr, Rezaei AR, Friehs GM, Okun MS, Shapira NA, Foote KD, Cosyns PR, Kubu CS, Malloy PF, Salloway SP, Giffakis JE, Rise MT, Machado AG, Baker KB, Stypulkowski PH, Goodman WK, Rasmussen SA, Nuttin BJ. Deep brain stimulation of the ventral internal capsule/ventral striatum for obsessive-compulsive disorder: worldwide experience [published online May 20, 2008]. *Mol Psychiatry*. doi:10.1038/mp.2008.55.
71. Mallet L, Polosan M, Jaafari N, Baup N, Welter ML, Fontaine D, du Montcel ST, Yelnik J, Chereau I, Arbus C, Raoul S, Aouizerate B, Damier P, Chabardes S, Czernecki V, Ardouin C, Krebs MO, Bardinet E, Chaynes P, Burbaud P, Cornu P, Derost P, Bougerol T, Bataille B, Mattei V, Dormont D, Devaux B, Verin M, Houeto JL, Pollak P, Benabid AL, Agid Y, Krack P, Millet B, Pelissolo A; STOC Study Group. Subthalamic nucleus stimulation in severe obsessive-compulsive disorder. *N Engl J Med*. 2008;359(20):2121-2134.
72. McCracken CB, Grace AA. High-frequency deep brain stimulation of the nucleus accumbens region suppresses neuronal activity and selectively modulates afferent drive in rat orbitofrontal cortex in vivo. *J Neurosci*. 2007;27(46):12601-12610.
73. Everitt BJ, Belin D, Economidou D, Pelloux Y, Dalley JW, Robbins TW. Neural mechanisms underlying the vulnerability to develop compulsive drug-seeking habits and addiction [review]. *Philos Trans R Soc Lond B Biol Sci*. 2008;363(1507):3125-3135.
74. Van Laere K, Nuttin B, Gabriels L, Dupont P, Rasmussen S, Greenberg BD, Cosyns P. Metabolic imaging of anterior capsular stimulation in refractory obsessive-compulsive disorder: a key role for the subgenual anterior cingulate and ventral striatum. *J Nucl Med*. 2006;47(5):740-747.
75. Guehl D, Benazzouz A, Aouizerate B, Cuny E, Rotge JY, Rougier A, Tignol J, Bioulac B, Burbaud P. Neuronal correlates of obsessions in the caudate nucleus. *Biol Psychiatry*. 2008;63(6):557-562.
76. Saxena S, Brody AL, Ho ML, Zohrabi N, Maidment KM, Baxter LR Jr. Differential brain metabolic predictors of response to paroxetine in obsessive-compulsive disorder versus major depression. *Am J Psychiatry*. 2003;160(3):522-532.
77. Surmeier DJ, Ding J, Day M, Wang Z, Shen W. D1 and D2 dopamine-receptor modulation of striatal glutamatergic signaling in striatal medium spiny neurons. *Trends Neurosci*. 2007;30(5):228-235.
78. Denys D, Zohar J, Westenberg HG. The role of dopamine in obsessive-compulsive disorder: preclinical and clinical evidence. *J Clin Psychiatry*. 2004;65(suppl 14):11-17.
79. Schwarz AJ, Gozzi A, Reese T, Bifone A. In vivo mapping of functional connectivity in neurotransmitter systems using pharmacological MRI. *Neuroimage*. 2007;34(4):1627-1636.
80. Pujol J, Torres L, Deus J, Cardoner N, Pifarre J, Capdevila A, Vallejo J. Functional magnetic resonance imaging study of frontal lobe activation during word generation in obsessive-compulsive disorder. *Biol Psychiatry*. 1999;45(7):891-897.
81. Purcell R, Maruff P, Kyrios M, Pantelis C. Neuropsychological deficits in obsessive-compulsive disorder: a comparison with unipolar depression, panic disorder, and normal controls. *Arch Gen Psychiatry*. 1998;55(5):415-423.
82. Greicius M. Resting-state functional connectivity in neuropsychiatric disorders. *Curr Opin Neurol*. 2008;21(4):424-430.
83. Harrison BJ, Pujol J, Lopez-Sola M, Hernandez-Ribas R, Deus J, Ortiz H, Soriano-Mas C, Yücel M, Pantelis C, Cardoner N. Consistency and functional specialization in the default mode brain network. *Proc Natl Acad Sci U S A*. 2008;105(28):9781-9786.
84. He BJ, Snyder AZ, Zempel JM, Smyth MD, Raichle ME. Electrophysiological correlates of the brain's intrinsic large-scale functional architecture. *Proc Natl Acad Sci U S A*. 2008;105(41):16039-16044.
85. Harrison BJ, Pujol J, Ortiz H, Fornito A, Pantelis C, Yücel M. Modulation of brain resting-state networks by sad mood induction. *PLoS One*. 2008;3(3):e1794.
86. Maia TV, Cooney RE, Peterson BS. The neural bases of obsessive-compulsive disorder in children and adults. *Dev Psychopathol*. 2008;20(4):1251-1283.
87. van den Heuvel OA, Remijnse PL, Mataix-Cols D, Vrenken H, Groenewegen HJ, Uylings HB, van Balkom AJ, Veltman DJ. The major symptom dimensions of obsessive-compulsive disorder are mediated by partially distinct neural systems [published online ahead of print October 24, 2008]. *Brain*. 2009;132(pt 4):853-868.
88. Shehzad ZE, Clare Kelly AM, Reiss PT, Gee DG, Gotimer K, Uddin LQ, Lee SH, Margulies DS, Krain Roy A, Biswal BB, Petkova E, Castellanos FX, Milham MP. The resting-brain: unconstrained yet reliable [published online February 16, 2009]. *Cereb Cortex*. doi:10.1093/cercor/bhn256.